Article

Not peer-reviewed version

The Anti-arthritic Activity of Diclofenac Lipid-Core Nanocapsules: Stereological Analysis Showing More Protection of Deep Joint Components

Nathalie Marte Ureña , Catiúscia Padilha De Oliviera , Silvia Guterres , Adriana Pohlmann * , Oscar Tadeu Ferreira da Costa * , Antonio Luiz Boechat *

Posted Date: 1 May 2023

doi: 10.20944/preprints202305.0018.v1

Keywords: Diclofenac; nanoformualtion; lipid-core nanocapsules; adjuvant arthritis; stereology; cartilage; synovial membrane

Article

The Anti-Arthritic Activity of Diclofenac Lipid-Core Nanocapsules: Stereological Analysis Showing More Protection of Deep Joint Components

Nathalie Marte Ureña [1], Catiúscia Padilha de Oliveira [2], Silvia Stanisçuaski Guterres [2], Adriana Raffin Pohlmann [2,*], Oscar Tadeu Ferreira da Costa [1,3] and Antonio Luiz Boechat [1,4,*]

[1] Programa de Pós-Graduação e Imunologia Básica e Aplicada, Universidade Federal do Amazonas, Brasil
[2] Programa de Pós-Graduação em Ciências Farmacêuticas, Faculdade de Farmácia, Universidade Federal do Rio Grande do Sul, Brasil
[3] Laboratório de Morfologia Quantitativa, Departamento de Morfologia, Instituto de Ciências Biológicas, Instituto de Ciências Biológicas, Universidade Federal do Amazonas, Brasil
[4] Laboratorio de Terapias Inovadoras, Departamento de Parasitologia, Instituto de Ciências Biológicas, Universidade Federal do Amazonas, Manaus, AM, Brasil
* Correspondence: authors: Adriana Raffin Pohlmann, Departamento de Química Orgânica, Instituto de Química, Universidade Federal do Rio Grande do Sul, Av. Bento Gonçalves 9500. PBOX 15003, CEP 91501-970, Porto Alegre, RS – Brasil. Tel.: +55-51-3308-7237, E-mail: adriana.pohlmann@ufrgs.br; Antônio Luiz Boechat, Departamento de Parasitologia, Instituto de Ciências Biológicas, Universidade Federal do Amazonas, Av. General Rodrigo Otávio, 3000 – Coroado I, CEP 69077-000, Manaus – AM – Brasil. Tel +55-92-8127-3388; E-mail: alboechat@ufam.edu.br .

Abstract: Introduction: Diclofenac is the most prescribed non-steroidal anti-inflammatory drug worldwide and used to reliev pain and inflammation for inflammatory arthritis. Diclofenac do not slows disease progression and cartialge damage of Rheuamtoid Arthritis individuals. Moreover, it associated with seriuos adverse effects even using regular dose regimens. Drug delivery systems can overcome this issues reducing adverse effects and optmizing efficacy**. Objectives:** to evaluate the activity of a lipid-core nanocapsule loaded of Diclofenac (DIC-LNC) in an experimental model of adjuvant-induced arthritis and its anti-arthritic properties at the joint components. **Methods:** The diclofenac nanoformulation was obtained by self-assembling methodology. The stereology analysis aproach was applied for morphological quantification of the volume, density and cellular profile count of the metatarsophalangeal joints of rats induced to adjuvant arthritis. Proinflamatory cytokines and biochemical profile was also obtained. **Results:** DIC-LNC is able to reduce arthitis compared to control group ($p<0.0001$) and DIC group ($p=0.009$). The TNF and IL1 cytokine as well as C-reative protein and Xanthine-oxidade were efficiently reduced by DIC-LNC. Additionally, DIC-LNC reduces synovites and condrocytes lossing compared to DIC ($p<0.05$)and control group ($p<0.05$). The synovial space volume was higher for DIC-LNC compared to DIC ($p<0.05$) and Control ($p<0.05$). These data are suggesting that DIC-LNC is showing anti-arthritic actvity preserving deep joint components. **Conclusion:** DIC-LNC is a promissing nanoformulation for clinical use, since is able to reduce joint inflamation and synovits, avoiding damage of cartilage and synovial space at advjuvant athrits. Further studies and developments are necessary to achieve future clinical use.

Keywords: diclofenac; nanoformulation; lipid-core nanocapsules; stereology; advuvant arthritis

1. Introduction

Non-steroidal anti-inflammatory drugs (NSAIDs) are the most prescribed medication to treat the pain and stiffness caused by Rheumatoid Arthritis (THAKUR et al., 2018). NSAIDs act via the inhibition of cyclooxygenase (COX) enzymes, blocking the production of prostanoids (prostaglandins [PGs], prostacyclin [PGI2], and thromboxane [TX]) which promote the pain, inflammation, and swelling of the inflamed tissue (HUNT et al., 2009; KU et al., 1986).

 doi:10.20944/preprints202305.0018.v1

Worldwide, Diclofenac is the most prescribed NSAID and can inhibit both isoforms of cyclooxygenase, COX-1, and COX-2 (ALTMAN et al., 2015). Diclofenac gives temporary relief for the symptoms of RA and is usually used in combination with Disease-modifying antirheumatic drugs (DMARDs) and glucocorticoids to relieve pain and inflammation. Non-steroidal anti-inflammatory drugs do not alter the progression of RA, and long-term use generates serious side effects (CROFFORD, 2013). Some of the adverse effects caused by the NSAIDs are esophagitis, peptic ulcer and gastrointestinal bleeding, chronic kidney disease, and death, especially by cardiovascular events. All of these side effects are caused by the poor selectivity for inflamed tissue (LANAS, 2009; CHAN et al., 2010).

To overcome this difficulty, nanotechnology can synthesize nanopharmaceuticals that delivers drugs to the targeted areas of inflammation, avoiding the possible side effects that drugs can cause to the system (PRASAD; O'MARY; CUI, 2015). Studies have demonstrated the enhanced anti-inflammatory activity and strong modulation of pro-inflammatory mediators that NSAIDs develop when used in nanostructure vehicles (CHIONG et al., 2013; TURK et al., 2013).

Lipid-core polymeric nanocapsules (LNC) are a type of polymeric nanoparticles constituted by a polymeric wall and an organo-gel core containing a dispersion of sorbitan monostearate in medium-chain triglycerides, stabilized by polysorbate 80 micelles (JÄGER et al., 2009; VENTURINI et al., 2011; FIEL et al., 2013). Recent studies have demonstrated diclofenac (acidform) loaded in lipid-core nanocapsules with high encapsulation efficiency by its distribution mainly in the polymer watt of the LNC, which can conduce to decrease the dose to elicit the necessary therapeutic activity and the side effects. The use of the LNC has shown many advantages like a decreased TNF-a, IL-1, and IL-6 level and increased the IL-10 level in the arthritis model using a LNC loaded indomethacin (BERNARDI et al., 2009)

In the effort to understand experimental arthritis, many studies have been using Stereology as a tool to quantify the morphological changes in these models (KELLER et al., 2012; KELLER et al., 2013). Stereology is defined as "The body of methods for the investigation of three-dimensional space when only two-dimensional sections through solid bodies or their projections on a surface are available" (EXNER, 2011). The application of Stereology provides the calculation of volume, density, and the counting of structures of one determinate object, through the analysis of two-dimension images. Helping to obtain accurate results with minimum bias through the evaluation of serial sections made from the object of interest (BOYCE et al., 2010). Studies have proven the efficacy that this technique has on the analysis of experimental models of arthritis (SILVA et al., 2004; THOTE et al., 2013). While conventional histology evaluates qualitative hallmarks of joint inflammation, stereology can provide accurate quantitative information to understand the treatment effects at key joint tissue components in experimental arthritis. We hypothesize that the diclofenac lipid-core nanocapsule aqueous formulation (DIC-LNC) preserves the chondrocytes, synovial space and diminishes synovitis of the arthritic joints. This work aims to evaluate, through stereological analysis, the anti-arthritic activity of DIC-LNC in an experimental model of arthritis.

2. Materials and Methods

2.1 Materials

Poly(ε-caprolactone) (PCL) (Mw = 65 000 g mol^{-1}) and sorbitan monostearate (Span 60®) were supplied by Sigma-Aldrich Co. Caprylic/capric triglyceride (CCT) was obtained from Delaware (Brazil) and polysorbate 80 was obtained from Brasquim (Brazil). Sodium diclofenac was obtained from Galena (Brazil). All other chemicals and solvents used were of analytical or pharmaceutical grades. All reagents were used as received.

2.2. Preparation of the lipid-core nanocapsules formulations

Firstly, the neutral diclofenac (acid form) was obtained by the methodology previously described (BECK et al 2004; OLIVEIRA et al 2013), in which the aqueous medium containing sodium diclofenac was acidified with 5 mol L^{-1} hydrochloric acid until turbidity was observed. So, that

 doi:10.20944/preprints202305.0018.v1

mixture was kept static to allow precipitation in a cooling bath and the precipitate obtained was filtered and recrystallized using water:ethanol (1:1, v/v). The colorless crystals were characterized by infrared spectroscopy (FT-IR 8300, Shimadzu) and presenting bands at swavelength number (cm-1) of 3300 (NH), 3200-2500 (OH), and 1710 (C=O).

The formulations containing or not diclofenac, denominated DIC-LNC and LNC, respectively, were prepared by interfacial deposition of preformed polymer methodology previously reported (VENTURINI et al 2011; OLIVEIRA et al 2013). The organic phases, at 40◦C, composed of acetone (27 mL), PCL (0.100 g), sorbitan monostearate (0.038 g), capric/caprylic triglyceride (0.160 g), and diclofenac (0,010 g), in the case of DIC-LNC, was poured into the aqueous phases (53 mL) containing polysorbate 80 (0.077 g) at 40 ◦C. The translucent solution was obtained instantaneously, and, afterward, acetone was removed and the solution was concentrated under reduced pressure at 40 ◦C. The final volume was adjusted to 10 mL in a volumetric flask.

2.3. Physicochemical characterization of the formulations

pH measurements

After preparation, the pH values of the formulations were determined without previous dilution by inserting the probe directly into the liquid formulation at room temperature. To this, a calibrated potentiometer B-474 (Micronal, Brazil) equipped with an Ag electrode/AgCl (Analion V620) was used.

Electrophoretic mobility and zeta potential

The zeta potential values were determined by meaduring th eelectropheretic mobility using the aforementioned Zetasizer® Nano ZS (Malvern Instruments Ltd., UK). The samples were diluted using 10 mmol L^{-1} NaCl aqueous solution (1:500, v/v) and the analysis was carried out at 25◦C.

Particle sizing

Laser diffraction

The granulometric profile of the DIC-LNC and LNC formulations were obtained by laser diffraction (Malvern Mastersizer® 2000, Malvern Instruments, UK) in the range of 40 nm to 2 mm. Each sample was directly added into the wet unit containing distilled water (about 150 mL), at room temperature. Formulations were analyzed using an obscuration between 2% and 8%. The volume-weighted mean diameter (D[4,3]) and the polydispersity of the distribution (Span, based on the diameters at 10%, 50%, and 90% of the cumulative size distribution) were determined.

Dynamic Light Scattering

Formulations were analyzed, at 25 °C, by dynamic light scattering (DLS) using ZetaSizer Nano ZS (Malvern Instruments Ltd., UK) to determine the distribution curve of diameters in the range from 1 nm to 5 μm, the mean hydrodynamic diameter (Dh), using the method of Cumulants, and the polydispersity index, using the relative variance in the particle size distribution. Formulations were diluted 500 times in ultrapure water (MilliQ®) and the intensity of the scattered light was analyzed at an angle of 173 ° providing the correlation curves, which were fit using a monoexponential model.

Nanoparticle tracking analysis

Nanoparticle Tracking Analysis (NTA) was performed using a NanoSight instrument (LM10, NanoSight Ltd., Amesbury, UK) after the formulations were diluted (5000 x) in pre-filtered ultrapure water (MilliQ®). By Brownian motion of the lipid-core nanocapsules, the hydrodynamic diameter (Dh), the median diameter (D50), the diameter at the 90th percentile (D90) under the cumulative size distribution, and the particle number density (PND) were obtained in real-time via a CCD camera. The video clips were captured over 60 s, at 21.6±0.5 °C and 0.96 ± 0.02 cP.

 doi:10.20944/preprints202305.0018.v1

Drug content and Encapsulation Efficiency

The DIC content of DIC-LNC was determined by a direct quantification using high-performance liquid chromatography (HPLC, Perkin Elmer S-200 with an S-200 injector) dotted of a UV-VIS detector () and mobile phase consisted of acetonitrile: water (65:35 v/v) adjusted to an apparent pH of 5.0±0.5 with 10% (v/v) acetic acid, with a flow rate of 1.0 mL min^{-1} and injection volume of the 20 µL[7]. The sample was diluted in acetonitrile in a volumetric flask and filtered with 0.45 µm membranes (Millipore, USA). The methodology presented proper linear regression, with r>0.999 in the interval used, 1-50 µg mL^{-1}, and demonstrated specificity, accuracy (99±1 %), repeatability, and precision (relative standard deviation <5%).

The encapsulation efficiency (EE%) was established by an indirect quantification using ultrafiltration-centrifugation by adding 300µL of the formulation, without previous dilution, in a Microcon® centrifugal filter device (10KDa, Millipore®, USA), after this the unit was centrifuged at 1844 xg (RCF) for 5 min using a centrifuge (Sigma® 1-14, Germany) and the ultrafiltrate was analyzed by HPLC with the method above described. The EE% was calculated from the difference between the total drug content (total concentration of the drug in the formulation) and the drug concentration in the ultrafiltrate (concentration of dissolved drug in the continuous phase) divided by the total content and multiplied by 100. All analyses were made in triplicate.

2.4. Animals

Twenty 8-week-old Lewis rats that weighed between 250 and 350 g were maintained in the biotherium at the Federal University of Amazonas (UFAM) and used in the experiment. The animals had access to water and food and were maintained in a light-controlled (12-hour light-dark cycle) and temperature-controlled (22°C) environment. They were allocated by simple randomization into four groups, four animals were maintained in each cage and one animal was kept alone for negative control. All experiments were performed with the approval of the Institutional Committee for Ethics in Animal Experiments under reference number 010/2010 (CEEA) UFAM.

2.5. Induction of arthritis by Freund's Complete Adjuvant and Experimental Design

The whole experimental design is showed at figure from Suplemmentary Material. The induction of arthritis was made through an intradermal injection on the tail of the rats with 0.1 mL of complete Freund's adjuvant (Difco, USA) after the inhalation of anesthesia with isoflurane, on the first day of the experiment. After the evidence of arthritis, the animals were allocated into four groups using simple randomization: Group 1: control (arthritic rats without treatment), Group 2: arthritis with empty LNC, Group 3: arthritis with a free solution of Diclofenac, and Group 4: arthritis with the nanoformulation DIC-LNC. On the Day 0 of the experiment, each treatment was initiated with an intraperitoneal injection of DIC, DIC-LNC and empty LNC, respectively for each group. The DIC and DIC-LNC dose was 3mg/kg/day. On day 28 of the experiment, the animals were killed by inhalation of isoflurane and blood was obtained by heart puncture.

2.6. Randomization, Blinding and Allocation Concealment

To allocate animals into a treatment group, a list of random numbers was used, and the animals were raffled by simple randomization (randomization.com.br). Allocation concealment was achieved by a codified random list produced by personnel that was not involved with experiment design nor conducting. All animal treatment assessments, biochemical markers, stereological and data analysis were conducted under blinding evaluation.

2.7. Edema volume and arthritis score of the hind paw

The volumes of the paws were measured on days 0, 7, 14, 21 and 28 of the experiments, with a digital plethysmometer (Insight®, Brazil). A blind evaluator assessed the paws volume measurements. The arthritis score was evaluated on the 28th day of the experiment. We scoring rat paws using an arthritis score as previously described (BOECHAT et al. 2015)

Preprints (www.preprints.org) | NOT PEER-REVIEWED | Posted: 1 May 2023 doi:10.20944/preprints202305.0018.v1

2.8. Quantification of cytokines and biochemical markers

With a CBA Flex Sets® (cytometry bead array) the serum levels of TNF-α, IL-1α and CRP were measured, following the manufacturer's instructions. To read the samples a FACSCalibur™ flow cytometer (BD Biosciences) was used. The quantity and mean fluorescence of the cytokines were calculated using BD FCAP Array™ Software (v 1.0.1; BD Biosciences). To calculate the serum levels of CRP, a Roche Hitachi Chemistry Analyzer and immunoturbidimetric assay (catalog number: 4956842190) was used following the manufacturer's instructions. Liver and renal toxicity were evaluated measuring glutamic oxaloacetic transaminase (TGO), glutamic pyruvic transaminase (TGP), gamma glutamyl transpeptidase (GGT, creatinine and blood urea nitrogen (BUN).

2.9. Stereological analysis

After the euthanasia, the left and right hind paws were removed and preserved in buffered formaldehyde 10% until the stereological analysis. Each paw was previously codified according to group allocation, and all stereological analyses were performed under allocation concealment strategy. The rat paws were washed in distilled water to remove any residue of formaldehyde. Then, the second digits of the paws were removed, since the articulation of interest was the metatarsophalangeal (MTP) of the second digit. The hair and skin of the digits were peeled for better absorption of the decalcifier substance. All the digits were kept in 10% Formic Acid for 48hrs until complete decalcification.

After this, they were washed in distilled water and dehydrated in an alcoholic series (70% and 96%), following resin embedding (Technovit 7100, Külzer-Heraeus, Germany). Each block containing the finger was kept in a stove at 50o C for 24 hrs.

After this, each block was positioned in an angle clock and randomly rotated to create different angles for sectioning, according to the principle of vertical sectioning (BADDELEY; GUNDERSEN; CRUZ-ORIVE, 1986). **Figure 1** shows the procedure used to obtain the vertical sections of the MTP joint. Ten to eleven sections (5 **µ**m thick) were taken with a constant distance (T) of 50 **µ**m for each block using a microtome (Leica RM 2145, Germany). The sections were stained with toluidine blue 0.5% (toluidine blue, 0.12 g; Na^+borate, 0.5 g; distilled H_2O, 100 mL) and basic fuchsin (basic fuchsin, 0.5 g and distilled H_2O, 100 mL). All these procedures for histological evaluation were described by Kiernan (1999).

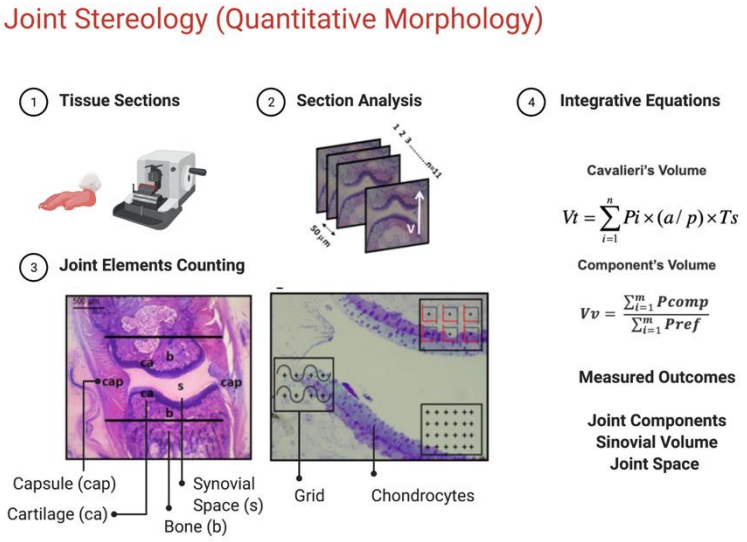

Figure 1. Methods used for stereological analysis. A. Sectioning level of the 2nd digit of the paw. B. Block of resin containing an MTP joint (longitudinal lines indicate the location of the knife during the microtomy. C. Generation of 50μm equidistant serial sections. Any section passing through the longitudinal plane of the finger will be a vertical section. D. Profile of a section used to determine

Preprints (www.preprints.org) | NOT PEER-REVIEWED | Posted: 1 May 2023 doi:10.20944/preprints202305.0018.v1

Cavalieri volume. In this magnification (8) the structures marked in the image are fully visible. The lines delimit the area investigated in this study limited by the border with the spongy bone E. Detail of the joint region used to estimate the volume density (point-counting system), surface area (counting system with points and curves) and number of chondrocyte profiles (counting system with frames and a central point). cap, capsule; b, bone; ca, cartilage; s, synovial space.

2.10. Determination of Cavalieri's Volume

The volume of the MTP joint was determined according to Cavalieri's principle (LOCKWOOD; EVES, 2007; GUNDERSEN; JENSEN, 1987). This principle is used when the precise calculation of any volume is needed. For this matter, all the serial sections of each block were digitized by the stereomicroscope (Leica EZ4D Digital System, Germany) and through the program of Imod 4.7/ stereology (KREMER; MASTRONARDE; MCINTOSH, 1996) a counting system of points was overlap on each section. The procedure consists of counting all the points hitting the MTP joint (defined by the limits of the capsule). The volume was estimated using the following formula:

$$\boldsymbol{V}\ (\boldsymbol{mm^3}) = \sum_{i=1}^{m} \boldsymbol{Pi} \times \boldsymbol{T} \times \boldsymbol{a/p}$$

Where, **V** was the absolute volume of the MTP joint; $\sum Pi$ was the sum of points hitting MTP; a/p was the area occupied by each central point (23470 μm²) and T (50 μm) was the distance between each section (GUNDERSEN; JENSEN, 1987).

2.11. Determination of Relative Volume

The percentage of each component within MTP was obtained by the Delesse principle (DELL'ISOLA; GUARASCIO; HUTTER, 2000). For this, microscopic fields of view within the joint were systematic, uniform and random sampled (magnification 200). Following the same procedure, a point counting system was superimposed over the images. The percentage of the volume occupied by each component in relation to the reference space (joint) was calculated as:

$$\boldsymbol{Vv\ (component, reference\ space)} = \frac{\sum_{i=1}^{m} \boldsymbol{Pcomp}}{\sum_{i=1}^{m} \boldsymbol{Pref}}$$

Where **Vv** was the volume density of articular component **∑Pcomp** was the sum of points hitting each component (capsule, synovial space, and synovial membrane) and **∑Pref** was the sum of points hitting the reference space (articular region) (HOWARD; REED, 1998). The percentage values obtained for each component were transformed into absolutes when multiplied by Cavalieri's volume of the joint, as seen on the next formula:

$$\boldsymbol{Absolut\ Volume(mm^3) = Vv\ x\ Cavalieri\ Volume}$$

2.12. Determination of Surface Area

The same images from the preview calculation of Delesse Volume were used to obtain the surface area of the articular cartilage and synovial membrane. Once again, a counting system with long cycloid curves and points was superimposed over the images. Each time a curve intercepted the edge of the cartilage in contact with the synovial space or the synovial membrane, it was counted. The same thing happened with the points that touched these structures. The density of the surface was calculated as:

$$\boldsymbol{Sv\ (mm^{-1})} = \frac{2\sum_{i=1}^{m} \boldsymbol{I}}{\sum_{i=1}^{m} \boldsymbol{Pi} \times \frac{\boldsymbol{l}}{\boldsymbol{p}}}$$

Where **Sv** stands for surface density, **∑I** is the sum of intersections, **∑P** is the sum of points, and **l/p** is the length of the test curve per grid point. The relative values obtained for each component were transformed into absolutes when multiplied by Cavalieri volume of the joint, see following formula:

$$\boldsymbol{Surface\ area\ (mm^{-1}) = Sv\ x\ Cavalieri\ Volume}$$

 doi:10.20944/preprints202305.0018.v1

2.13. Counting number of cellular profiles

To determine the number of chondrocytes profiles present in articular cartilage, we used a 2-D quantification technique. The counting system consists of six frames (2700,28 μm²), and each frame contains a reference point. The counting frames consisted of a solid forbidden line and a dashed acceptance line. Only the nucleus of the cells that appear inside the counting frame, and did not touch the exclusive line were counted. The number of cells was expressed as profiles/mm² and calculated with the following formula:

$$\boldsymbol{Nv} = \frac{\sum_{i=1}^{m} \boldsymbol{Q-}}{\boldsymbol{Nf\ X\ Af}}$$

Where: **∑Qchon** was the cellular profile number of chondrocytes; **∑N frames** were the sum of all the analyzed molding frames; **Aframe** was the area of the molding frame.

2.14. Statistical Analysis

Data were expressed as means and standard deviations. The results are expressed as the means and standard deviations, and a 95% confidence interval was used. One-way or Two-way ANOVA were used to compare the means, and a Sidak's test for multiple comparisons or linear test for trend was used for post hoc analysis. The Mann-Whitney test was used when the Barllet analysis did not observe normality. Linear regression and curve-fitting with non-linear polynomial regression were applied to study the effects of the different MTX preparations on cytokine levels in the blood and synovial culture cells. A significance level of α=0.05 was adopted, and all p-values were two-tailed. The level of significance used was 5%. For stereology analysis, the variance was expressed as the coefficient of error (CE) for each parameter evaluated (V, Vv and Sv). The accuracy of the Cavalieri volume estimates was determined according to (CRUZ-ORIVE 1999),

$$\mathbf{CE} = \left[\mathbf{0,0724} \times \frac{\boldsymbol{B}}{\sqrt{\boldsymbol{A}}} \times \frac{\sqrt{\boldsymbol{n}}}{(\sum_{i=1}^{m} \boldsymbol{Pi})^{\frac{3}{2}}}\right]^{\frac{1}{2}}$$

Where CE indicates the coefficient of error for Cavalieri's volume determination; $\frac{\boldsymbol{B}}{\sqrt{\boldsymbol{A}}}$ Indicates the variance in the count on the sections (shape coefficient) and depends on the morphological complexity of the structure; n represents the number of sections evaluated and is the number of points counted on the sections.

3. Results

3.1 Preparation of DIC-LNC dispersed in water

Lipid-core nanocapsules loadingdiclofenac, DIC-LNC, and blank lipid-core nanocapsules, LNC, presented white-bluish opalescent liquids with Tyndall effect (visual aspect). The granulometric profile of the DIC-LNC and LNC (**Figure 2**) obtained by laser diffraction (LD) analysis showed unimodal distributions with D[4,3] below 204±46 nm (Span < 1.7) for both formulations. No micrometer particle population was formed whatever the formulations, containing or not diclofenac. Table 3 summarizes all values obtained by different techniques for DIC-LNC and LNC. These formulations were also analyzed by dynamic light scattering (DLS) to improve accuracy in the nanoscale range measurements and showed hydrodynamic mean diameter (Dh) below 170 nm with narrow polydispersity indexes (PDI<0.1). Besides the DLS, the hydrodynamic diameters of the formulations also were obtained by nanoparticle tracking analysis (NTA). The NTA technique determines the diameters from individual particles by tracking and sizing them by recording the positional changes due to their Brownian movement. The formulations showed Dh between 182 and 196, D90 below the 309 nm and particle number density between 4.76 x 10^{12} and 4.98 x 10^{12} nanocapsules mL^{-1} (Table 1).

After assessing the size distribution, the drug loading and encapsulation efficiency of the DIC-LNC were evaluated showing drug content of 1.09±0.10 mg mL^{-1} and encapsulation efficiency of

Preprints (www.preprints.org) | NOT PEER-REVIEWED | Posted: 1 May 2023 doi:10.20944/preprints202305.0018.v1

100%. The pH and the zeta potential were determined and no significant difference between DIC-LNC and LNC were observed.

Table 1. Characterization of the formulations by potentiometry, laser diffraction, dynamic light scattering and nanoparticle tracking analysis.

	LNC	DIC-LNC
Potentiometry		
pH	5.43±0.24	5.39±0.16
Laser diffraction		
D[4.3] (nm)	153±10	204±46
Span	1.4±0.2	1.7±0.1
Dynamic Light Scattering		
Dh (nm)	170±13	166±13
PDI	0.06±0.02	0.08±0.02
Electrophoretic mobility		
Zeta Potential (mV)	-13±6	-11±2
Nanoparticle tracking analysis		
Dh (nm)	182±9	196±14
D50 (nm)	173±13	186±2
D90 (nm)	257±10	309±9
PND (x10^{12} particles mL^{-1})	4.98±0.25	4.76±0.78

Note. Data are expressed as mean ± standard deviation. Abbreviations: LNC, blank lipid-core nanocapsules; DIC-LNC, acid diclofenac loaded lipid-core nanocapsules; D[4.3], volume-weighted diameter average; Dh, hydrodynamic diameter; PDI, polydispersity index; D50, median diameter; D90, the diameter at the 90th percentile; PND, particle number density.

3.2. DIC-LNC reduces edema formation at the hind paws

The **Figure 3** shows edema formation (**Panel 2A** and **2B**) and treatments effect over hind paw volume and arthritis score (**Panel C**). DIC-LNC reduces paw volume compared to control (p < 0.00010.05) and DIC 9p = 0.05) at 28th days, mean reduction of -0.848mL (95% CI -1.80 to -0.51).

Preprints (www.preprints.org) | NOT PEER-REVIEWED | Posted: 1 May 2023 doi:10.20944/preprints202305.0018.v1

Moreover, the treatment effect of DIC-LNC appears to be early on arthritis reduction at 21st day compared to DIC (mean reduction -0.338mL 95%CI -0.54 to -0.19, p< 0.0001).

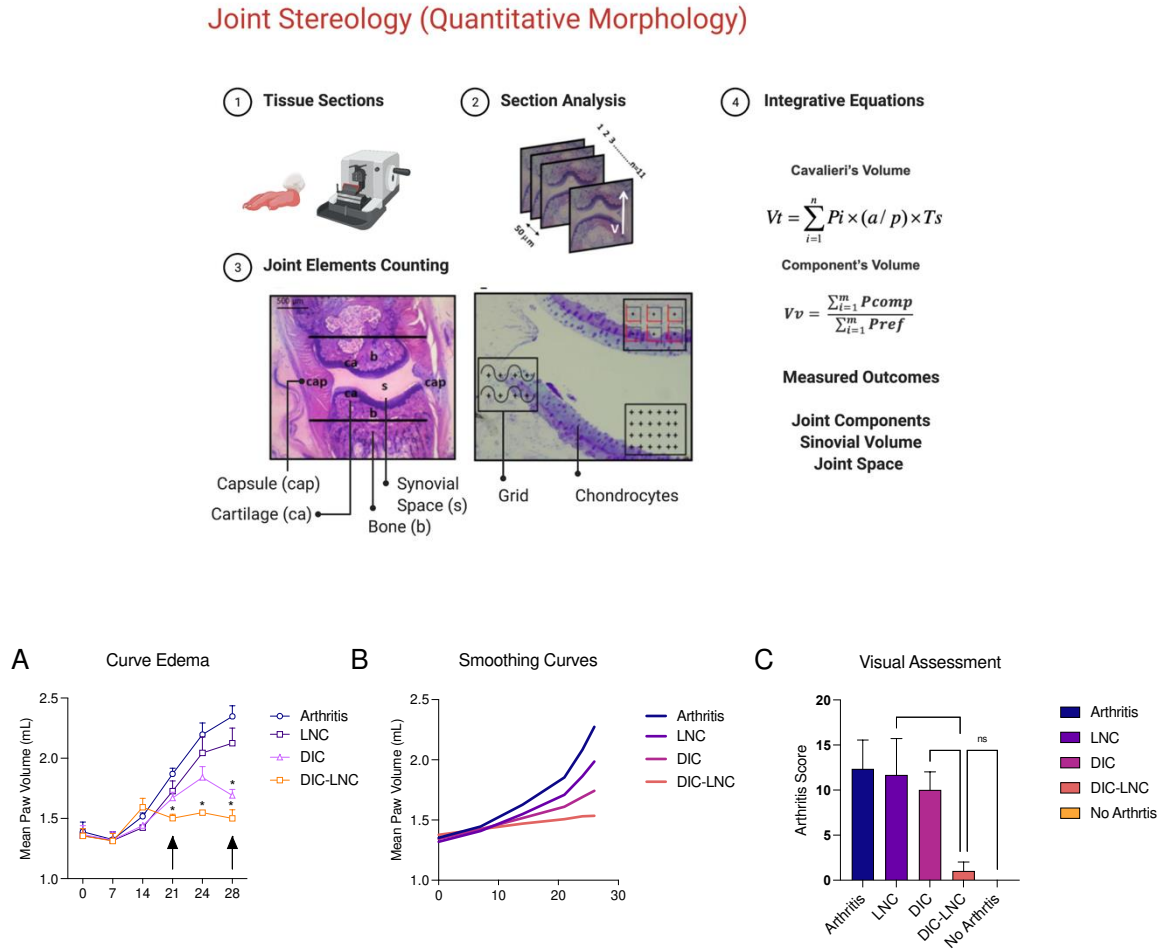

Figure 3. Arthritis evaluation and Scores for twenty-eighty days. A. Arthritis kinetics, the black arrows indicate the maximum effects observed; B – Edema curve with smoothing techniques and C – Arthritis score. ** (p<0.05).

3.3. DIC-LNC reduces the serum levels of proinflammatory cytokines and CRP

The serum levels of TNF-α were significantly lower in the DIC-LNC group compared with the DIC group using Sidak's test (p < 0.0001, **Figure 4A**). The serum IL1α levels were similar for both groups when the comparison was performed using a Tukey's test (p = 0.778); however, the linear test for trend indicated a significant trend (p = 0.0001). The CRP levels were also lower for the DIC-LNC group compared with DIC (Mann-Whitney test, p = 0.0286, **Figure 4B**).

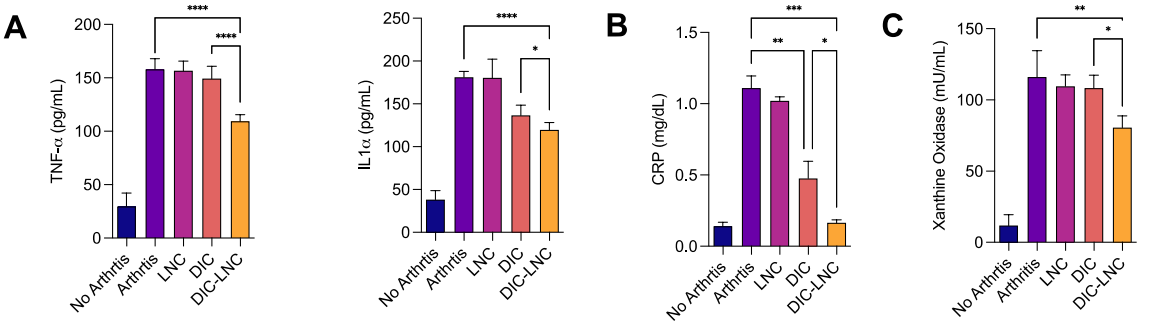

Preprints (www.preprints.org) | NOT PEER-REVIEWED | Posted: 1 May 2023 doi:10.20944/preprints202305.0018.v1

Figure 4. Serum Inflammatory Markers on day twenty-eight of the experiment. A – Quantification of the proinflammatory cytokines TNF-α and IL-1α. B – Serum levels of CRP for the DIC and DIC-LNC groups and C – xanthine-oxidase as an oxidative stress marker. .

3.4. Absence of liver and renal toxicity with DIC-LNC

To evaluate the liver and kidney toxicity liver enzymes and renal function markers were evaluated (**Figure 5**, **Panel A** and **B**). It was observed that the use of the DIC-LNC did not alter the serum levels of these enzymes ($p>0.05$) at the doses used at this research, suggesting no liver toxicity (**Figure 5, Panel A**). Following the same protocol, the serum levels of creatinine and blood urea nitrogen (BUN) were measured to evaluate renal toxicity (**Figure 5, Panel B**). It was also observed that the use of the DIC-LNC did not alter the serum levels of BUN nor creatinine, in comparison with the other treatments ($p>0.05$).

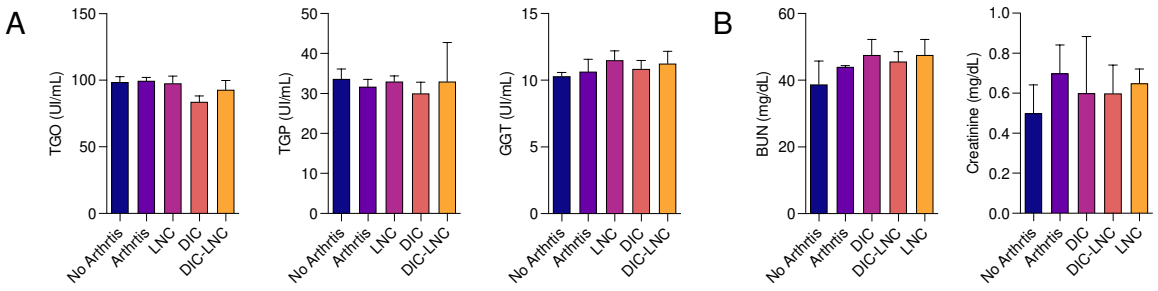

Figure 5. Liver and Kidney Toxicity biochemical markers. A) Liver biochemical markers (TGO, TGP, GGT) of all five groups (Ul/mL). B) Kidney biochemical markers (BUN, CRE) for all five groups (mg/dL).

3.5. Cavalieri's Volume of MTP joints

Figure 6 shows the influence of the number of sections on the efficiency and accuracy of determining the Cavalieri volume of the MTP joint. In a pilot study, a rat's paw finger was histologically processed into resin and thoroughly sectioned to produce 28 sections that were evaluated for the determination of volume according to Cavalieri. A reductive process was applied to show the relationship between the smallest number of sections associated with a low CE. Our results indicated that the use of 10 sections is as accurate as the use of 28 sections and, in addition, it is much more efficient.

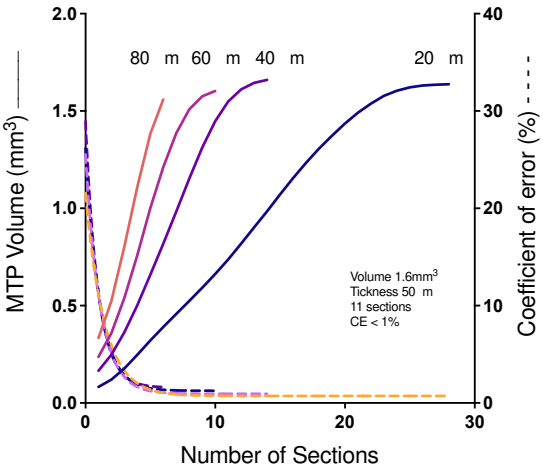

 doi:10.20944/preprints202305.0018.v1

Figure 6. Relationship between Cavalieri's volume and the coefficient of error. Demonstration of the relation between the number of serial sections (x axis), the volume of Cavalieri (right y axis) and the coefficient of error (left y axis). Continuous lines indicate the volume and dotted lines represent the respective error coefficient. Blue indicates 28 serial sections equidistant 20 mm; Green indicates 14 40 mm equidistant serial sections; Purple indicates 10 equidistant 60 mm serial sections and red indicates 16 equidistant 80 mm serial sections.

Table 2 and **Figure 7** (**Panel A**) present the results of MTP joint volume. The volume was higher on the Arthritis group when compared with the Diclofenac ($p = 0.0007$) and DIC-LNC group ($p < 0.0001$). Most important, the DIC-LNC presented differences with the Diclofenac group ($p = 0.023$), showing the DIC-LNC formulation was more efficient to control edema formation. These results demonstrate that DIC-LNC had an effective diminution of joint volume with values similar to the No Arthritis group.

Table 2. MTP Joint volume and Density of its different components.

	Volume (mm^3)					
Groups	Joint	Cartilage	Bone	**Capsule**	**Synovial Space**	**Synovial Membrane**
Arthritis	3.02±0.08[1]	0.50±0.10	1.20±0.05	0.97±0.14	0.16±0.01	0.06±0.04
LNC	2.80±0.32[1]	0.36±0.08	1.08±0.16	0.89±0.15	0.17±0.01	0.04±0.01
Diclofenac	2.46±0.12[2]	0.34±0.03	1.02±0.12	0.67±0.02	0.19±0.02	0.03±0.00
Diclofenac-LNC	2.10±0.10[3]	0.21±0.01	0.75±0.05	0.58±0.02	0.26±0.01	0.02±0.00
No Arthritis	1.95±0.05[4]	0.23±0.03	0.61±0.06	0.52±0.03	0.41±0.03	0.01±0.05

Note. Data are expressed as mean ± standard deviation. ANOVA and Turkey's multiple comparisons ($p< 0.001$). Abbreviations: LNC, blank lipid-core nanocapsules.

3.6. Density of the joint components and Absolute volume

Table 2 and **Figure 7** (**Panel B**) summarize the results obtained from the calculation of the relative volume of each component of MTP. The Arthritis group presented an elevated volume of cartilage (arthritis vs DIC $p = 0.002$; arthritis vs DIC-LNC $p < 0.0001$), bone (arthritis vs DIC $p = 0.142$; arthritis vs DIC-LNC $p = 0.0002$), capsule (arthritis vs DIC $p = 0.142$; arthritis vs DIC-LNC $p < 0.0002$) and synovial membrane (arthritis vs DIC $p = 0.0003$; arthritis vs DIC-LNC $p = 0.0001$), when compared with Diclofenac and DIC-LNC groups respectively. It is interesting to note that cartilage volume expansion is reflecting both damage of cartilage content by inflammation and marginal bone and cartilage formation.

The treatment with DIC-LNC preserved the synovial space ($p = 0.007$) and diminished the volume of cartilage ($p = 0.031$), bone ($p = 0.01,6$) and synovial membrane ($p = 0.0009$, Brown-Forsyte ANOVA test due to unequstandardard deviation and Dunnet's T3 for multiple comparisons) when compared with the Diclofenac group (**Figure 7C**). Demonstrating that DIC-LNC causes a reduction of joint inflammation.

Preprints (www.preprints.org) | NOT PEER-REVIEWED | Posted: 1 May 2023 doi:10.20944/preprints202305.0018.v1

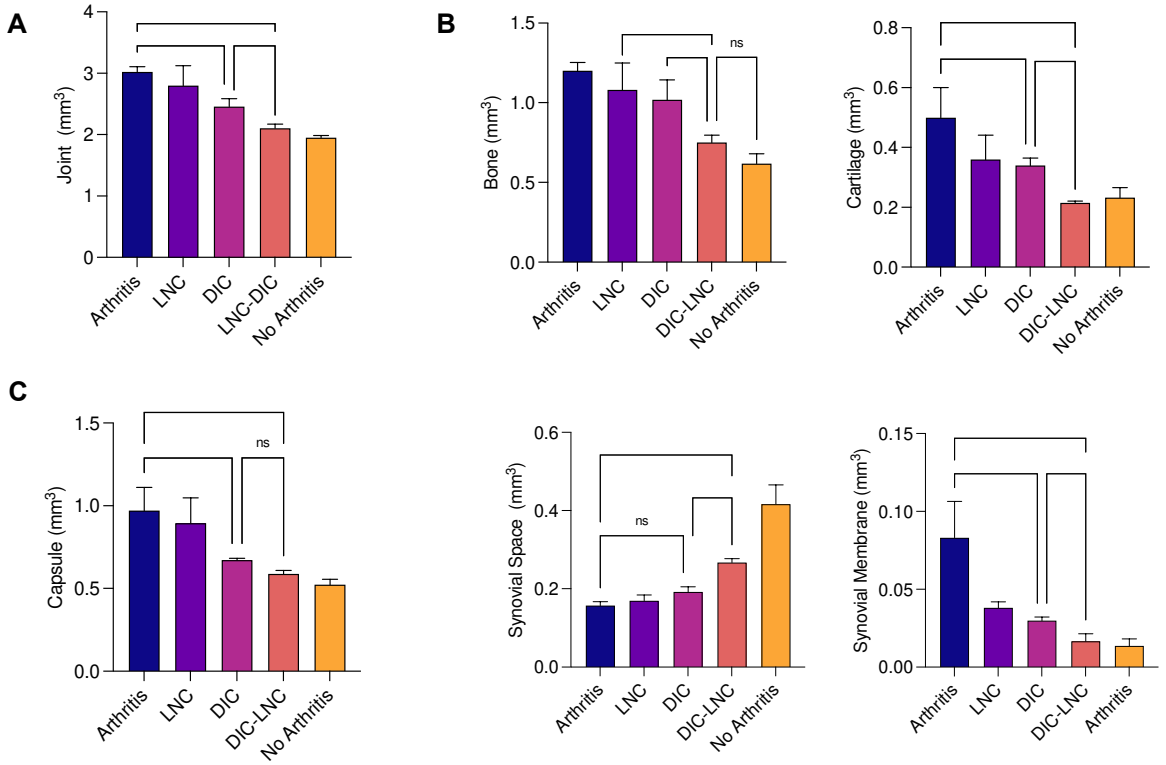

Figure The volumelume of the MTP joint and each component. A) MTP joint volume of all treated groups. B) Absolute volume of the components of MTP of each treated group and C) Volume of Capsule, Synovi,al Space and Synovial Membrane. ANOVA significance p <0.05.

3.7. Surface area of MTP joints

Table 3 and **Figure 8** are showing the rethe sults of surface area of the cartilage and synovial membrane of MTP. The erosions at cartilage surface usually are reflected by a higher surface area measurement. On the other hand, a higher surface area is observed due to inflamed synovial villosities. Thus, the Arthritis group presented the highest surface area of cartilage (arthritis vs DIC $p = 0.001$; arthritis vs DIC -LNC $p = 0.0001$) and synovial membrane (arthritis vs DIC $p = 0.006$; arthritis vs DIC-LNC $p < 0.0001$) when compared with the Diclofenac and DIC-LNC groups, respectively. As shown in **Figure 8**, the treatment with DIC-LNC restored the values of cartilage ($p = 0.015$) and synovial membrane ($p = 0.045$) in comparison with the Diclofenac group.

Table 3. Surface area and Cellular count of MTP.

	Surface Área (mm²)		Cellular Count (cell/mm²)		
Groups	**Cartilage**	**Synovial Membrane**	**Chondrocytes**	**Isogenous Groups**	**Total chondrocytes**
Arthritis	38.25±4.32	14.22±2.43	1416±126.3	80.55±8.77[1]	1517±54.30
LNC	29.09±3.75	10.42±1.92	1543±49.92	111.5±4.51[2]	1701±91.96

Preprints (www.preprints.org) | NOT PEER-REVIEWED | Posted: 1 May 2023 doi:10.20944/preprints202305.0018.v1

Diclofenac	27.87±3.31	10.06±0.53	1627±95.61	161.1±11.84[3]	1849±16.73
Diclofenac-LNC	20.45±1.58	8.19±0.22	1894±47.00	226.8±20.5[4]	2095±52.33
No Arthritis	19.45±1.28	6.71±1.40	2208±217.4	297.9±19.5[5]	2367±225.8

Note: Data are expressed as mean ± standard deviation.

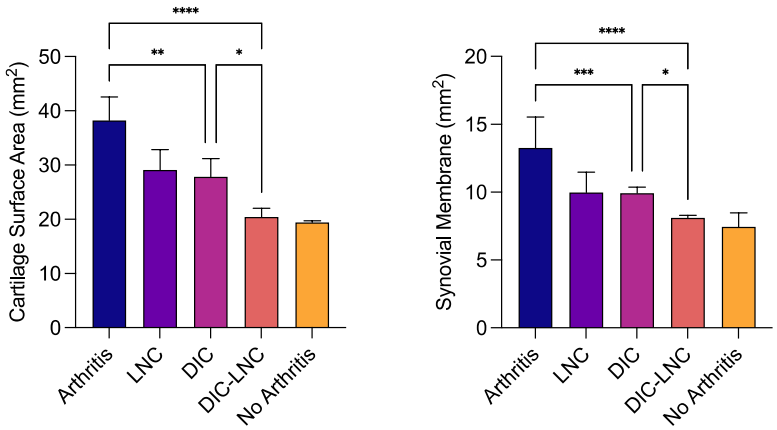

Figure 8. The surface area of MTP. The left panel presents the surface area of the cartilage. The right panel presents the surface area of the synovial membrane. ANOVA significance p <0.05.

3.8. Quantification of chondrocytes

Table 3 and Figure 9 summarize the results of chondrocyte count. The No Arthritis group presented the highest number of total chondrocytes. On the other hand, the Arthritis group presented the lowest count of chondrocytes (p = 0.084, p = 0.002) when compared with Diclofenac and DIC-LNC groups. The Arthritis group also presented a reduction in the number of isogenous groups (p < 0.001; p < 0.001) and the total number of chondrocytes (p = 0.004; p <0.001) when compared with Diclofenac and DIC-LNC groups. The DIC-LNC group presented higher numbers of isogenous groups (p < 0.001) and total chondrocytes (*p*=0.004) when compared with the Diclofenac group.

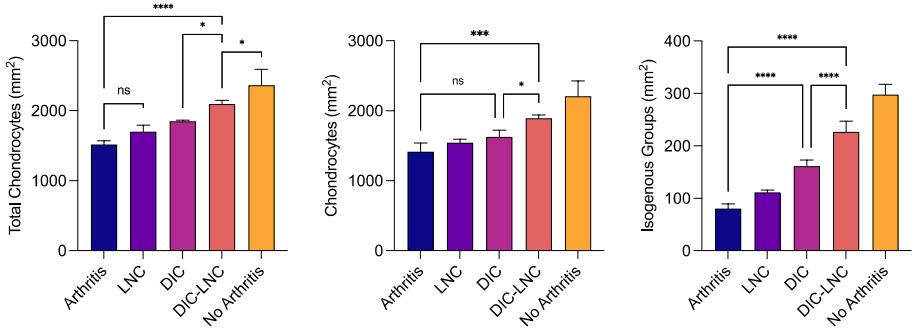

Figure 9. Cellular profile count of MTP chondrocytes. The left panel shows the total number of chondrocytes count. The middle panel shows the number of isolated chondrocytes. The right panel shows the number of isogenous groups of chondrocytes, present after mitosis. ANOVA significance p < 0.05.

 doi:10.20944/preprints202305.0018.v1

4. Discussion

In this project we aimed to evaluate, through stereological analysis, the anti-arthritic activity of DIC-LNC in an experimental model of arthritis. To this end, a lipid core nanocapsule, containing diclofenac, was formulated by interfacial deposition of polymer method. We demonstrated at this work that these diclofenac-loaded lipid-core nanocapsules (DIC-LNC) are able to reduce paw inflammation and cytokine production, preventing synovitis, synovial space and cartilage losses by morphologic quantitative methods. Together, these effects strongly support an anti-arthritic effect for DIC-LNC.

For both formulations, DIC-LNC and LNC, the polydispersity index values were lower than 0.1 indicating narrow size distributions of the nanocapsules showed by unimodal size distribution profiles. Moreover, DIC-LNC presented mean diameter of 204±46nm, pH of 5.39±0.16 and Dh of 196 nm and D90 of 309 nm obtained by NTA. These physicochemical parameters show that these nanocapsules are suitable for intravenous circulation. Lipid-core nanocapsules (LNC) have demonstrated to be effective formulations to entrapped pharmaceuticals (FROZZA et al., 2010) and to deliver drugs in specific areas of inflammation like multiform glioblastoma (BERNARDI et al., 2009), neuroinflammation (BERNARDI et al., 2010) and chronic inflammation (CRUZ et al., 2006). Furthermore, LNCs have been proven to be non-toxic to animal experimental models (BULCÃO et al., 2014). Thus, these nanomaterials are efficient in delivering pharmaceuticals to specific areas while minimizing the side effects of the drugs.

Although the success of DMARDS use for rheumatoid arthritis treatment under a treat-to-target approach, pain and inflammation are still challenges at clinical practice (ZANG & LEE, 2018). Proinflammatory cytokines like tumor necrosis factor-alpha (TNF-α), interleukin-1-beta (IL-1β), interleukin-6 (IL-6) and interleukin-17 (IL-17) can rise the peripheral nociceptive neurons sensitization (SCHAIBLE 2014). These cytokines are locally produced by proliferated synovial cells, like macrophages and fibroblasts, and activated T lymphocytes cells at joint inflamed synovia (FIRESTEIN; MCINNES 2017). When proliferated by inflammatory signals, the synovial membrane cells infiltrate joint components and allow cartilage destruction, bone erosion, and joint space narrowing (MCINNES et al 2017). Eicosanoids production at inflamed synovia are both related to pain sensitization and joint inflammation (CROFFORD et al 1994) and are stimulated by inflammatory cytokines (ANDERSON et al 1996; MARTEL-PELLETIER et al 2004).

It has been well known that pro-inflammatory cytokines especially enhance the expression of cyclooxygenase-2 (COX-2) and metalloproteinases (MMP) in human synovial fibroblasts (RASF) (GITTER et al 1989; CROFFORD et al. 1994). Cyclooxygenase and leukotriene inhibition reduce cartilage erosion and bone erosion for both adjuvant arthritis and collagen-induced arthritis (GILROY et al 1989; ANDERSON et al 1996; 2009) Moreover, recent investigations showed that RA patients with optimized treatment highly express cyclooxygenase at the synovial membrane (KOROTKOVA; JAKOBSSON, 2014). When the human cyclooxygenase-2 gene is silenced on cultured synovial cells of rheumatoid arthritis patients, there is a reduction of prostaglandin E2 (PGE2), vascular endothelial growth factor (VEGF), IL-1β and TNF-α (LENG et al 2018). Taking together, these data may account for those anti-arthritic effects demonstrated for DIC-LNC over conventional diclofenac in experimental arthritis in our work.

With the use of Stereological analysis, it has been proven that there is an augmentation of bone formation in arthritic experimental models. A group of researchers analyzed the bone surface of the joints of arthritic mice. They observed that the mineralizing surfaces of the bone were higher on arthritic mice ($p < 0.001$) when compared with the control group (KRARUP KELLER et al., 2012). This may be explained by the production of TNF-α that promotes the differentiation of osteoclasts in the arthritic joints, which leads to invasion of inflammatory tissue, imbalance of bone resorption/formation and later remodeling of the bone (DIARRA et al., 2007).

In our study, we observed a higher volume of the bone in arthritic joints when compared with the other groups. Also, the experimental model of arthritis used in the project, Adjuvant-Induced Arthritis (AIA), is an aggressive representation of RA that leads to ankylosis and joint malformation. AIA is characterized by inflammation of soft tissue, marked bone loss and periosteal new bone

formation (CAI et al., 2006). This data may indicate that the arthritic joints were in the process of joint remodeling.

One marked manifestation of Rheumatoid Arthritis is inflammation of the synovial membrane (SMOLEN; ALETAHA; MCINNES, 2016). In the synovial lining, there is an increase in the activity of fibroblast-like synoviocytes, which produce prostaglandins (PGs) and metalloproteinases (MMPs) that contribute to the destruction of the joint (SMOLEN et al., 2007). Synovitis has been related to the production of TNF-α, IL-17, IL-6, and IL-1. This group of proinflammatory cytokines cause hyperplasia of the synovia and angiogenesis by the activation of macrophages, dendritic cells, T and B lymphocytes (CHOY, 2012).

Synovial membrane augmentation of RA patients was studied using stereological analysis. Researchers observed a significant increase of the synovia when compared with the control group (ARTACHO-PÉRULA et al., 1994). Also applying stereological analysis, Kristensen et. al, studied the synovial proliferation of arthritic rabbits. The team observed that the arthritic joints of rabbits presented the highest scores of synovial proliferation and thickness when compared with the control group (KRISTENSEN et al., 2008). Our results also show an increase in the volume of the synovial membrane of arthritic joints when compared with the other groups. Making these results coherent with the literature.

Drug nanoencapsulation may increase drug-tissue interactions raising the drug tissue concentration or modified drug biodistribution (FRANK et al 2015). For instance, the ketoprofen-loaded polymeric nanocapsules are able to cross the blood-brain barrier by a passive transport after in vivo treatment of glioblastoma in rats (SILVEIRA et al 2013). When nanocapsules are given orally, the adhesion on mucosae improves the performance of the drug nanosystems. Thus, the interaction of indomethacin ethyl-ester lipid-core nanocapsules with the gastrointestinal tract acting as a mucoadhesive drug reservoir (CATTANI et al 2010). Of note, nanocapsules are internalized together with the encapsulated substance into the endosomal compartment or in the micronucleus. After that, the drug is then released by simple diffusion, by polymer enzymatic degradation, or by redox-responsive degradation of the polymer.

Recently network metanalysis showed that diclofenac is more likely to control pain, improving physical function with similar adverse effects to other compared NSAID (van WALSEM et al 2015). The diclofenac therapeutic effect for arthritis is largely related to its synovial fluid concentration (FOWLER et al 1983). The synovial bioavailability of diclofenac, on its turn, may be limited by oral absorption and first-pass hepatic metabolism (FOWLER et al 1983; YUAN et al 2017). A high plasma concentration of diclofenac is a key pharmacokinetic element to reach synovia. After 6 hours a single intravenous 75mg injection, the diclofenac synovial concentration corresponds to 166% of plasma levels (FOWLER et al. 2017). However, after the first-pass metabolism, approximately only 50% of the drug reaches the systemic circulation in an unchanged form, and this extensive metabolism accounts for diclofenac having poor oral bioavailability (KASPEREK et al 2017). Moreover, after an oral diclofenac intake, large interindividual differences in plasma concentrations were observed (HELLMS et al 2019). These individual variations may account for therapeutic inefficiency, due to low serum concentrations, and for the observed adverse reactions, when higher serum levels were achieved. As we previous reported diclofenac nanocapsules formulations achieves higher serum concentrations compared to sodium diclofenac oral solution with a lower drug-induced organ damages (GUTERRES et al. 2001).

5. Conclusions

Our results demonstrate the anti-arthritic activity of DIC-LNC. Using stereological analysis we calculated the articular volume of MTP and its components, the surface area of the cartilage and synovium and 2-D cellular count profile of chondrocytes. We demonstrated that the lipid-core nanocapsule reduced the joint synovitis and preserved the articular cartilage, chondrocytes and synovial space. DIC-LNC is a innovative and promising nanoformulation for future treatment of RA and other inflammatory joint diseases. However, more analysis needs to be made regarding the effects of nanocapsules in humans.

Funding: The authors thank the Brazilian Agencies: Coordination for the Improvement of Higher Education Personnel (CAPES), National Council of Technological and Scientific Development (CNPq) and Research Support Foundation of the State of Rio Grande do Sul (FAPERGS). INCT-NANOFARMA [São Paulo Research Foundation (FAPESP, Brazil) Grant #2014/50928-2 and CNPq Grant # 465687/2014-8]; CNPq/PQ (305343/2019-0); and PRONEX/FAPERGS/CNPq 12/2014 #16/2551-0000467-6. Financial support was also provided in the form of grants from Fundação de Amparo à Pesquisa do Estado do Amazonas (FAPEAM) (POSGRAD Program #008/2021 and #005/2022), Conselho Nacional de Desenvolvimento Científico e Tecnológico (CNPq) and Coordenação de Aperfeiçoamento de Pessoal de Nível Superior (CAPES) (PNPD Program). Nathalie Marte Ureña have scholarships from FAPEAM, CAPES and CNPq (Masters and PhD students). The funders had no role in the study's design, data collection and analysis, the decision to publish or the preparation of the manuscript.

Ethics approval and consent to participate: All necessary aproval from ethical committee was receiveid (Institutional Committee for Ethics in Animal Experiments under reference number 010/2010 CEEA-UFAM).

Consent for publication: Not applicable.

Availability of data and materials: All data and materials of this manuscript are already available at this final manuscript version.

Competing Interests: None.

References

ALTMAN, R. et al. Advances in NSAID development: Evolution of diclofenac products using pharmaceutical technology. Drugs, v. 75, n. 8, p. 859-877, 2015.

ANDERSON, G. D. et al. Selective inhibition of cyclooxygenase (COX)-2 reverses inflammation and expression of COX-2 and interleukin 6 in rat adjuvant arthritis. Journal of Clinical Investigation, v. 97, n. 11, p. 2672–2679, 1 jun. 1996.

ANDERSON, G. D. et al. Combination therapies that inhibit cyclooxygenase-2 and leukotriene synthesis prevent disease in murine collagen induced arthritis. Inflammation Research, v. 58, n. 2, p. 109-117, 2009.

ARTACHO-PÉRULA, E. et al. Stereological analysis of the synovial membrane in rheumatic disorders: diagnostic value of volume-weighted mean nuclear volume estimation. Histopathology, v. 25, n. 4, p. 357–363, 1 out. 1994.

ASQUITH, D. L. et al. Animal models of rheumatoid arthritis. European Journal of Immunology, v. 39, n. 8, p. 2040–2044, 2009.

BADDELEY, A. J.; GUNDERSEN, H. J. G.; CRUZ-ORIVE, L. M. Estimation of surface area from vertical sections. Journal of Microscopy, v. 142, n. 3, p. 259–276, 1 jun. 1986.

BECK, R. C. R.; POHLMANN, A. R.; GUTERRES, S. S. Nanoparticle-coated microparticles: Preparation and characterization. Journal of Microencapsulation, v. 21, n. 5, p. 499–512, ago. 2004.

BERNARDI, A. et al. THEMED SECTION : MEDIATORS AND RECEPTORS IN THE RESOLUTION OF INFLAMMATION Effects of indomethacin-loaded nanocapsules in experimental models of inflammation in rats. British Journal of Pharmacology, v. 158, n. 4, p. 1104–1111, 2009.

BERNARDI, A. et al. Protective effects of indomethacin-loaded nanocapsules against oxygen-glucose deprivation in organotypic hippocampal slice cultures: Involvement of neuroinflammation. Neurochemistry International, v. 57, n. 6, p. 629–636, 1 nov. 2010.

BOECHAT, A. L. et al. Methotrexate-loaded lipid-core nanocapsules are highly effective in the control of inflammation in synovial cells and a chronic arthritis model. International Journal of Nanomedicine, v. 10, n. 1, p. 6603–6614, 2015.

BOYCE, R. W. et al. Design-based stereology: introduction to basic concepts and practical approaches for estimation of cell number. Toxicologic pathology, v. 38, n. 7, p. 1011-1025, 2010.

BRAND, D. D.; LATHAM, K. A.; ROSLONIEC, E. F. Collagen-induced arthritis. Nature Protocols, v. 2, n. 5, p. 1269-1275, 2007.

BULCÃO, R. P. et al. In vivo toxicological evaluation of polymeric nanocapsules after intradermal administration. European Journal of Pharmaceutics and Biopharmaceutics, v. 86, n. 2, p. 167–177, fev. 2014.

CAI, X. et al. The comparative study of Sprague-Dawley and Lewis rats in adjuvant-induced arthritis. Naunyn-Schmiedeberg's Archives of Pharmacology, v. 373, n. 2, p. 140–147, 2006.

CATTANI, V. B. et al. Lipid-core nanocapsules restrained the indomethacin ethyl ester hydrolysis in the gastrointestinal lumen and wall acting as mucoadhesive reservoirs. European Journal of Pharmaceutical Sciences, v. 39, p. 116–124, 2010.

CHAN, F. K. L. et al. Celecoxib versus omeprazole and diclofenac in patients with osteoarthritis and rheumatoid arthritis (CONDOR): A randomised trial. The Lancet, v. 376, n. 9736, p. 173–179, 2010.

CHIONG, H. S. et al. Cytoprotective and enhanced anti-inflammatory activities of liposomal piroxicam formulation in lipopolysaccharide-stimulated RAW 264.7 macrophages. International Journal of Nanomedicine, v. 8, p. 1245–1255, 2013.

CHOY, E. Understanding the dynamics: Pathways involved in the pathogenesis of rheumatoid arthritis. Rheumatology (United Kingdom), v. 51, n. sup 5, p. 3-11, 2012.

CROFFORD, L. J. Use of NSAIDs in treating patients with arthritis. Arthritis Research and Therapy, v. 15, n. sup 3, p. 1-10, 2013.

CRUZ-ORIVE, L. M. Precision of Cavalieri sections and slices with local errors. Journal of Microscopy, v. 193, n. 3, p. 182–198, 1999.

CRUZ, L. et al. Physico-chemical characterization and in vivo evaluation of indomethacin ethyl ester-loaded nanocapsules by PCS, TEM, SAXS, interfacial alkaline hydrolysis and antiedematogenic activity. Journal of Nanoscience and Nanotechnology. v. 6, n. 9-10, p. 3154-3162, 2006.

DA SILVEIRA, E. F. et al. Ketoprofen-loaded polymeric nanocapsules selectively inhibit cancer cell growth in vitro and in preclinical model of glioblastoma multiforme. Investigational New Drugs, v. 31, p. 1424–1435, 2013.

DAYER, J. M.; CHOY, E. Therapeutic targets in rheumatoid arthritis: the interleukin-6 receptor. Rheumatology (Oxford, England), v. 49, n. 1, p. 15-24, 2010.

DELL'ISOLA, F.; GUARASCIO, M.; HUTTER, K. A variational approach for the deformation of a saturated porous solid. A second-gradient theory extending Terzaghi's effective stress principle. Archive of Applied Mechanics, 2000.

DIARRA, D. et al. Dickkopf-1 is a master regulator of joint remodeling. Nature Medicine, v. 13, n. 2, p. 156–163, 21 fev. 2007.

DOLATI, S. et al. Utilization of nanoparticle technology in rheumatoid arthritis treatment. Biomedicine and Pharmacotherapy, v. 80, p. 30-41, 2016.

EMERY, P. et al. IL-6 receptor inhibition with tocilizumab improves treatment outcomes in patients with rheumatoid arthritis refractory to anti-tumour necrosis factor biologicals : results from a 24-week multicentre randomised placebo-controlled trial. Annals of the Rheumatic Diseases, v. 67, n. 11, p. 1516-1523, 2008.

EXNER, H. E. STEREOLOGY AND 3D MICROSCOPY: USEFUL ALTERNATIVES OR COMPETITORS IN THE QUANTITATIVE ANALYSIS OF MICROSTRUCTURES. Image Analysis & Stereology, v. 23, n. 2, p. 73–82, 2011.

FC, B. et al. - The PREMIER study: A multicenter, randomized, double-blind clinical trial of. Arthritis Rheum, v. 54, p. 26-37, 2006.

FIEL, L. A. et al. Variable temperature multiple light scattering analysis to determine the enthalpic term of a reversible agglomeration in submicrometric colloidal formulations: A quick quantitative comparison of the relative physical stability. Colloids and Surfaces A: Physicochemical and Engineering Aspects, v. 431, n. 8, p. 93–104, 20 ago. 2013.

FIRESTEIN, G. S.; MCINNES, I. B. Immunopathogenesis of Rheumatoid Arthritis. Immunity, v. 46, n. 2, p. 183-196, 2017.

FOWLER, P. D. et al. Plasma and synovial fluid concentrations of diclofenac sodium and its major hydroxylated metabolites during long-term treatment of rheumatoid arthritis. European Journal of Clinical Pharmacology, v. 25, n. 3, p. 389–394, 1983.

FRANK, L. A. et al. Improving drug biological effects by encapsulation into polymeric nanocapsules. Nanomedicine and Nanobiotechnology, v. 7, n. 5, p. 623–639, 1 set. 2015.

FROZZA, R. L. et al. Characterization of trans-resveratrol-loaded lipid-core nanocapsules and tissue distribution studies in rats. Journal of Biomedical Nanotechnology, v. 6, n. 6, p. 694-703, 2010.

GHARAGOZLOO, M.; MAJEWSKI, S.; FOLDVARI, M. Therapeutic applications of nanomedicine in autoimmune diseases: From immunosuppression to tolerance induction. Nanomedicine: Nanotechnology, Biology, and Medicine, v. 11, n. 4, p. 1003-1018, ,2015.

GILROY, D. W. et al. The effects of cyclooxygenase 2 inhibitors on cartilage erosion and bone loss in a model of Mycobacterium tuberculosis-induced monoarticular arthritis in the rat. Inflammation, v. 22, n. 5, p. 509-519, 1998.

GITTER, B. D. et al. Characteristics of human synovial fibroblast activation by IL-1 beta and TNF alpha. Immunology, v. 66, p. 196–200, 1989.

GUTERRES, SS et al. Gastrointestinal Tolerance Following Oral Adminstration of Spray-Dried Diclofenac-loaded Nanocapsules and Nanospheres. STP Pharma Sciencies 11(3) 229-233, 2001.

GOUVEIA, V. M. et al. Non-biologic nanodelivery therapies for rheumatoid arthritis. Journal of Biomedical Nanotechnology, v. 11, n. 10, p. 1701-1721, 2015.

GULATI, M.; FARAH, Z.; MOUYIS, M. Clinical features of rheumatoid arthritis. Medicine (United Kingdom), v. 46, n. 4, p. 211-215, 2018.

GUNDERSEN, H. J. G. et al. Some new, simple and efficient stereological methods and their use in pathological research and diagnosis. APMIS, v. 96, p. 379–394, 2009.

GUNDERSEN, H. J. G.; JENSEN, E. B. The efficiency of systematic sampling in stereology and its prediction. Journal of Microscopy, v. 147, n. 3, p. 229–263, 1987.

HELLMS, S. et al. Single-dose diclofenac in healthy volunteers can cause decrease in renal perfusion measured by functional magnetic resonance imaging. Journal of Pharmacy and Pharmacology, v. 71, n. 8, p. 1262–1270, 2019.

HOBSON, D. W. Nanotechnology. In: Comprehensive Biotechnology, Second Edition, 2011.

HOWARD, C. V; REED, M. G. Unbiased Stereology Three-dimensional Measurement in Microscopy Second Edition, p. 17, 1998

HUNT, R. H. et al. Myths and facts in the use of anti-inflammatory drugs. Annals of Medicine, v. 41, n. 6, p. 423-437, 2009.

JÄGER, E. et al. Sustained release from lipid-core nanocapsules by varying the core viscosity and the particle surface area. Journal of Biomedical Nanotechnology, v. 5, n. 1, p. 130–140, fev. 2009.

KASPEREK, R. et al. Pharmacokinetics of diclofenac sodium and papaverine hydrochloride after oral administration of tablets to rabbits. Acta Poloniae Pharmaceutica - Drug Research, 2015.

KELLER, K. K. et al. Bone Formation and Resorption Are Both Increased in Experimental Autoimmune Arthritis. PLoS ONE, v. 7, n. 12, p. 1–7, 27 dez. 2012.

KELLER, K. K. et al. Improving efficiency in stereology: A study applying the proportionator and the autodisector on virtual slides. Journal of Microscopy, v. 251, n. 1, p. 68–76, 2013.

KOROTKOVA, M.; JAKOBSSON, P. J. Persisting eicosanoid pathways in rheumatic diseasesNature Reviews RheumatologyNature Publishing Group, , 2014.

KRISTENSEN, K. D. et al. Quantitative histological changes of repeated antigen-induced arthritis in the temporomandibular joints of rabbits treated with intra-articular corticosteroid. Journal of Oral Pathology and Medicine, v. 37, n. 7, p. 437–444, 2008.

KROENKE, K.; KREBS, E. E.; BAIR, M. J. Pharmacotherapy of chronic pain: a synthesis of recommendations from systematic reviews. General Hospital Psychiatry, 2009.

KU, E. C. et al. Effect of diclofenac sodium on the arachidonic acid cascade. The American Journal of Medicine, v. 80, n. 4 SUPPL. 2, p. 18–23, 28 abr. 1986.

LANAS, A. Nonsteroidal antiinflammatory drugs and cyclooxygenase inhibition in the gastrointestinal tract: A trip from peptic ulcer to colon cancer. American Journal of the Medical Sciences, 2009.

LENG, P. et al. Effects of human cyclooxygenase-2 gene silencing on synovial cells of rheumatoid arthritis mediated by lentivirus. Artificial Cells, Nanomedicine and Biotechnology, v. 46, n. sup3, p. S274–S280, 12 nov. 2018.

LI, P.; SCHWARZ, E. M. The TNF-?? transgenic mouse model of inflammatory arthritisSpringer Seminars in Immunopathology, 2003.

LOCKWOOD, E. H.; EVES, H. Great Moments in Mathematics (Before 1650). The Mathematical Gazette, 2007.

MA, M. H. Y.; KINGSLEY, G. H.; SCOTT, D. L. A systematic comparison of combination DMARD therapy and tumour necrosis inhibitor therapy with methotrexate in patients with early rheumatoid arthritis. Rheumatology, 2009.

MCINNES, I. B.; SCHETT, G. Cytokines in the pathogenesis of rheumatoid arthritisNature Reviews Immunology, 2007.

NOGUEIRA, E. et al. Folate-targeted nanoparticles for rheumatoid arthritis therapyNanomedicine: Nanotechnology, Biology, and Medicine, 2016.

OLIVEIRA, C. P. et al. An algorithm to determine the mechanism of drug distribution in lipid-core nanocapsule formulations. Soft Matter, v. 9, n. 4, p. 1141–1150, 2013.

PHAM, C. T. N. Nanotherapeutic approaches for the treatment of rheumatoid arthritis. Wiley Interdisciplinary Reviews: Nanomedicine and Nanobiotechnology, 2011.

PRASAD, L. K.; O'MARY, H.; CUI, Z. Nanomedicine delivers promising treatments for rheumatoid arthritisNanomedicine, 2015.

RAYCHAUDHURI, S. et al. Five amino acids in three HLA proteins explain most of the association between MHC and seropositive rheumatoid arthritis. Nature Genetics, 2012.

SILVA, M. D. et al. Quantitative analysis of micro-CT imaging and histopathological signatures of experimental arthritis in rats. Molecular Imaging, v. 3, n. 4, p. 312–318, 2004.

SMOLEN, J. S. et al. New therapies for treatment of rheumatoid arthritis. Lancet, v. 370, p. 1861–1874, 2007.

SMOLEN, J. S.; ALETAHA, D.; MCINNES, I. B. Rheumatoid arthritis. The Lancet, v. 388, n. 10055, p. 2023–2038, 2016.

STATKUTE, L.; RUDERMAN, E. M. Novel TNF antagonists for the treatment of rheumatoid arthritis. Expert Opinion, v. 19, n. 1, p. 105–115, 2010.

THAKUR, S. et al. Novel drug delivery systems for NSAIDs in management of rheumatoid arthritis: An overview. Biomedicine and PharmacotherapyElsevier Masson SAS, , 1 out. 2018.

THOTE, T. et al. Localized 3D analysis of cartilage composition and morphology in small animal models of joint degeneration. Osteoarthritis and Cartilage, v. 21, n. 8, p. 1132–1141, 2013.

TRELLE, S. et al. Cardiovascular safety of non-steroidal anti-inflammatory drugs: Network meta-analysis. BMJ, 2011.

TURK, C. T. S. et al. Formulation and Optimization of Nonionic Surfactants Emulsified Nimesulide-Loaded PLGA-Based Nanoparticles by Design of Experiments. AAPS PharmSciTech, v. 15, n. 1, p. 161–176, 2013.

UHLIG, T.; MOE, R. H.; KVIEN, T. K. The Burden of Disease in Rheumatoid Arthritis. PharmacoEconomics, v. 32, n. 9, p. 841–851, 2014.

VAN DE LAAR, M. Pain Treatment in Arthritis-Related Pain: Beyond NSAIDs. The Open Rheumatology Journal, v. 6, p. 320–330, 2012.

VAN WALSEM, A. et al. Relative benefit-risk comparing diclofenac to other traditional non-steroidal anti-inflammatory drugs and cyclooxygenase-2 inhibitors in patients with osteoarthritis or rheumatoid arthritis: A network meta-analysis. Arthritis Research and Therapy, 2015.

VENTURINI, C. G. et al. Formulation of lipid core nanocapsules. Colloids and Surfaces A: Physicochemical and Engineering Aspects, v. 375, n. 1–3, p. 200–208, 5 fev. 2011.

WEISSIG, V.; PETTINGER, T. K.; MURDOCK, N. Nanopharmaceuticals (part 1): products on the market. International journal of nanomedicine, 2014.

WENG, H. H. et al. Equivalent responses to disease-modifying antirheumatic drugs initiated at any time during the first 15 months after symptom onset in patients with seropositive rheumatoid arthritis. Journal of Rheumatology, 2010.

YUAN, J. et al. A pharmacokinetic study of diclofenac sodium in rats. Biomedical Reports, v. 7, n. 2, p. 179–182, 1 ago. 2017.

ZHANG, Q. et al. Neutrophil membrane-coated nanoparticles inhibit synovial inflammation and alleviate joint damage in inflammatory arthritis. Nature Nanotechnology, 2018.